Available online at www.sciencedirect.com
ScienceDirect
Mathematics and Computers in Simulation 79 (2008) 1071–1077
MATHEMATICS AND COMPUTERS IN SIMULATION
www.elsevier.com/locate/matcom

The effect of uniaxial stress on band structure and electron mobility of silicon

E. Ungersboeck [a,*], W. Gös [b], S. Dhar [a], H. Kosina [a], S. Selberherr [a]

[a] *Institute for Microelectronics, TU Wien, Gusshausstrasse 27–29/E360, 1040 Wien, Austria*
[b] *Christian Doppler Laboratory for TCAD in Microelectronics, Gusshausstrasse 27–29/E360, 1040 Wien, Austria*

Received 28 September 2007; accepted 1 October 2007
Available online 22 October 2007

Abstract

The band structure of silicon (Si) under arbitrary stress/strain conditions is calculated using the empirical nonlocal pseudopotential method. The method is discussed with a special focus on the strain induced breaking of crystal symmetry. It is demonstrated that under general stress the relative movement of the sublattices has a prominent effect on the conduction band masses. This displacement, which cannot be determined from macroscopic strain, is extracted from ab initio calculations. The transport properties of strained Si are investigated by solving the semi-classical Boltzmann equation using the Monte Carlo (MC) method. It is shown that the change of the electron effective mass induced by uniaxial stress has to be included in accurate models of the electron mobility.

PACS: 71.15.Dx; 71.70.Fk; 72.20.Fr

Keywords: Band structure; Empirical pseudopotential method; Uniaxial strain/stress; Monte Carlo method; Low-field mobility

1. Introduction

To continue improvement of CMOS device performance, strain techniques have become widely adopted in logic technologies starting with the 90 nm technology generation. Especially process induced uniaxial stress became established, because it increases mobility of both n-channel and p-channel MOSFETs [7,10,24].

While the mobility enhancement in biaxially strained Si has often been subject to theoretical investigations, a thorough theoretical analysis of the technologically more relevant case, where process-induced uniaxial stress is applied along the channel direction, is missing. Although published experimental results [4,8,18,25] suggested a stress induced modification of the *electron* effective mass, the mobility enhancement induced by strain is frequently understood from the lifting of the degeneracy of the Δ_6 conduction band valleys only [5]. In this work, the stress induced effective mass change is calculated and its effect on the mobility enhancement in Si is demonstrated. The paper is organized as follows: Section 2 describes the band structure calculations that predict the observed effective mass change. The analysis starts with the calculation of the strain tensor arising from uniaxial stress along an arbitrary direction, and the stress-induced reduction of the crystal symmetry is explained. Furthermore, important details concerning the generalization of the

* Corresponding author.
E-mail address: ungersboeck@iue.tuwien.ac.at (E. Ungersboeck).

0378-4754/$32.00
doi:10.1016/j.matcom.2007.10.004

empirical nonlocal pseudopotential method (EPM) for arbitrary strain are highlighted. In Section 3 the simulation scheme for the electron mobility of Si is highlighted. The results of band structure calculations and the electron mobility enhancement of uniaxially stressed Si are presented in Section 4.

2. Band structure calculations

The empirical pseudopotential method (EPM) was developed in the 1960s [12,21] as a way to solve Schrödinger's equation for bulk crystals without knowing exactly the potential experienced by an electron in the lattice. It is frequently used to calculate the full band structure of semiconductors, because it is efficient and requires only a small number of fitting parameters [1].

The EPM was later adapted to incorporate strain effects introduced by epitaxy. The band structure calculations for epitaxially grown $Si_{1-x}Ge_x$layers on $Si_{1-y}Ge_y$ substrates with (1 0 0) orientation were reported in [22], and for other orientations in [2,26]. In the following we present how general strain conditions can be incorporated into the EPM with a focus on strain arising from uniaxial stress.

2.1. Strain from uniaxial stress

While epitaxial strain for arbitrary substrate orientations can be calculated according to [6], here the calculation of the strain tensor resulting from a uniaxial stress of magnitude P along an arbitrary direction is given. Analysis begins by adopting a coordinate system (x', y', z') in which the x'-axis is parallel to the stress direction yielding a stress tensor with only one non-zero component, $\sigma'_{xx} = P$.

This system is related to the principal coordinate system (x, y, z) of the primary crystallographic axes of the semiconductor by a rotation $\bar{U}$

$$\bar{U}(\theta, \phi) = \begin{pmatrix} \cos\theta\,\cos\phi & -\sin\phi & \sin\theta\,\cos\phi \\ \cos\theta\,\sin\phi & \cos\phi & \sin\theta\,\sin\phi \\ -\sin\theta & 0 & \cos\theta \end{pmatrix}. \tag{1}$$

The angles θ and ϕ are the polar and azimuthal angles of the stress direction relative to the axes of the principal system. The stress in the principal system can be calculated from

$$\sigma_{ij} = U_{\alpha i} U_{\beta j} \sigma'_{\alpha\beta}. \tag{2}$$

The strain tensor can be calculated by inversion of Hooke's law $\varepsilon_{ij} = S_{ijkl}\sigma_{kl}$, where S_{ijkl} denotes the elastic compliance tensor and ε_{ij} the strain tensor. Using the above relations in Si the strain tensor for uniaxial stress of magnitude P applied along [1 1 0] reads

$$\bar{\varepsilon}_{[1\,1\,0]} = \frac{P}{2} \begin{pmatrix} s_{11} + s_{12} & \dfrac{s_{44}}{2} & 0 \\ \dfrac{s_{44}}{2} & s_{11} + s_{12} & 0 \\ 0 & 0 & 2s_{12} \end{pmatrix},$$

where $s_{11} = 0.00769$, $s_{12} = -0.00214$, and $s_{44} = 0.012559$ are the three compliance constants of Si in units of GPa^{-1} [19].

2.2. Symmetry considerations

The number of symmetry elements $P(\Gamma)$ at the center of the Brillouin zone (BZ) of the strained lattice determines the volume of the irreducible wedge, $\Omega_{\text{irred}} = \Omega_{\text{BZ}}/P(\Gamma)$. For stress along ⟨1 0 0⟩, ⟨1 1 1⟩, and ⟨1 1 0⟩, $P(\Gamma)$ can be shown to be 16, 12, and 8, respectively, while for stress along an arbitrary direction, the lattice is invariant only to inversion, yielding $P(\Gamma) = 2$. In this case the energy bands have to be calculated on half of the first BZ. The irreducible volume of the strained crystal can be split into wedges, forming the irreducible zone of the unstrained crystal. Stress along a ⟨1 0 0⟩ axis yields the same symmetry reduction as biaxial strain resulting from epitaxial growth on a (0 0 1) oriented wafer. The energy bands have to be calculated in a volume consisting of three irreducible wedges of the unstrained

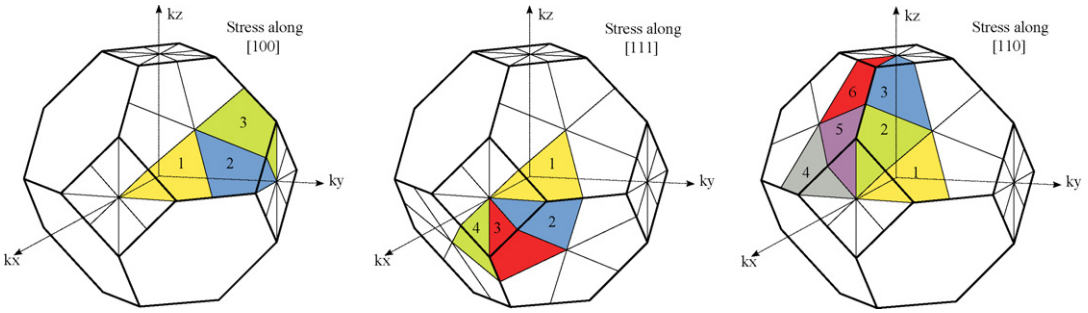

Fig. 1. Irreducible volume of the first BZ of Si being uniaxially stressed along three high-symmetry directions.

lattice. Stress along ⟨1 1 1⟩ or ⟨1 1 0⟩ further reduces symmetry. The corresponding irreducible volumes are shown in Fig. 1. If uniaxial stress is applied along ⟨1 1 1⟩, the irreducible zone contains four wedges, and six wedges for stress along ⟨1 1 0⟩. The symmetries can be exploited for models based on the full band structure, since energy bands have to be calculated and stored only in the irreducible volume of the first BZ.

Si band structure calculations were performed with a parameter set provided in [22]. Results are in good agreement with the cited work for unstrained and biaxially strained Si. To handle general strain conditions, some modifications in the band structure calculation are implied: (i) The strained direct lattice vectors have to be calculated from the strain tensor to determine the strained reciprocal lattice vectors, which are used for the diagonalization of the Hamiltonian matrix and the normalizing volume of the strained unit cell. (ii) Since the local pseudopotential form factors enter the calculation at the strained reciprocal lattice vectors, an interpolation of the pseudopotential is required. Several expressions have been proposed in [3,22]. We follow [22] using $k_F = 1.66(2\pi/a_0)$ for the Fermi wave vector. (iii) Generally, the macroscopic strain is not sufficient to determine the absolute positions of the two atomic positions in the bulk unit cell. An additional displacement has to be accounted for in terms of an internal strain parameter [11]. For stress along [1 1 0] the additional displacement along the z-axis is given by

$$u_z = -\frac{\xi}{2}\frac{(1+\varepsilon_{xx})\varepsilon_{xy}}{1+\varepsilon_{zz}}a_0, \tag{3}$$

where a_0 denotes the Si lattice constant (see Fig. 2). For the determination of the internal strain parameter ξ we performed calculations with the ab initio total-energy and molecular-dynamics program VASP (Vienna ab initio simulation program) developed at the Institut für Materialphysik of the Universtität Wien [13–16] using the PAW pseudopotentials [17]. A value of 0.5 was extracted, which is very close to previous theoretical calculations of Nielson [20], who extracted a value of 0.53.

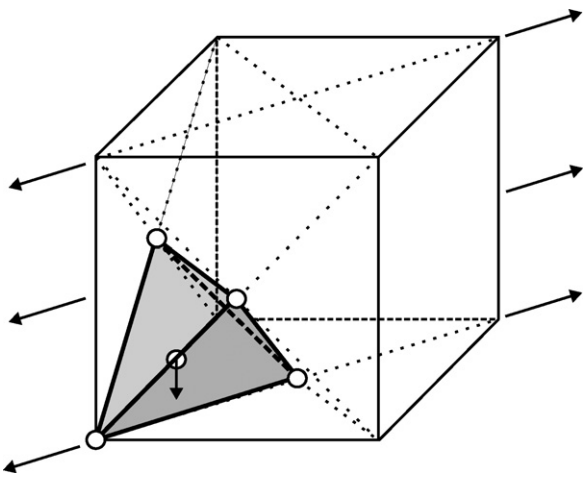

Fig. 2. Sketch of Si unit cell uniaxially stressed along ⟨1 1 0⟩. The center atom undergoes an additional displacement to minimize the overall energy stored in the strained lattice.

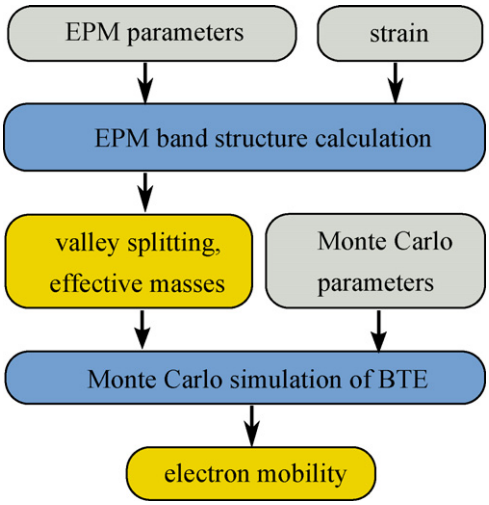

Fig. 3. Flowchart presenting the computational scheme for the calculation of the electron mobility.

3. Simulation of electron mobility

The electron mobility in bulk Si is analyzed by solving the semi-classical Boltzmann transport equation using a Monte Carlo (MC) method [9]. For this purpose the Vienna Monte Carlo simulator VMC [27] was developed, offering simulation algorithms for both bulk semiconductors and one-dimensional devices with models based on both analytical bands (ABMC) and the full band structure (FBMC). VMC provides a comprehensive set of scattering models including phonon scattering, ionized impurity scattering, alloy scattering, and impact ionization.

The ABMC simulator was extended to enable the simulation of bulk electron mobility of uniaxial ⟨1 1 0⟩ stressed Si. The overall simulation scheme is depicted in Fig. 3. Note that the strain induced shifts of the Δ-valleys and the change of the effective masses resulting from the band structure calculations are used as input parameters for the subsequent MC simulation.

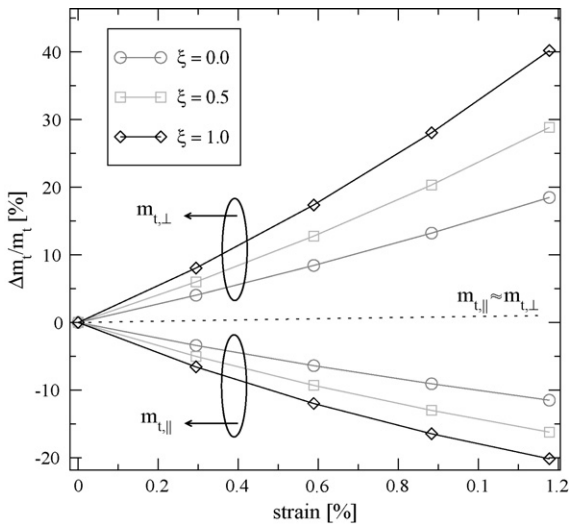

Fig. 4. Effect of biaxial tensile strain (dotted line) and uniaxial ⟨1 1 0⟩ tensile stress (solid lines with symbols) on the in-plane masses of the Δ_2 valley. Strain is given in stress direction.

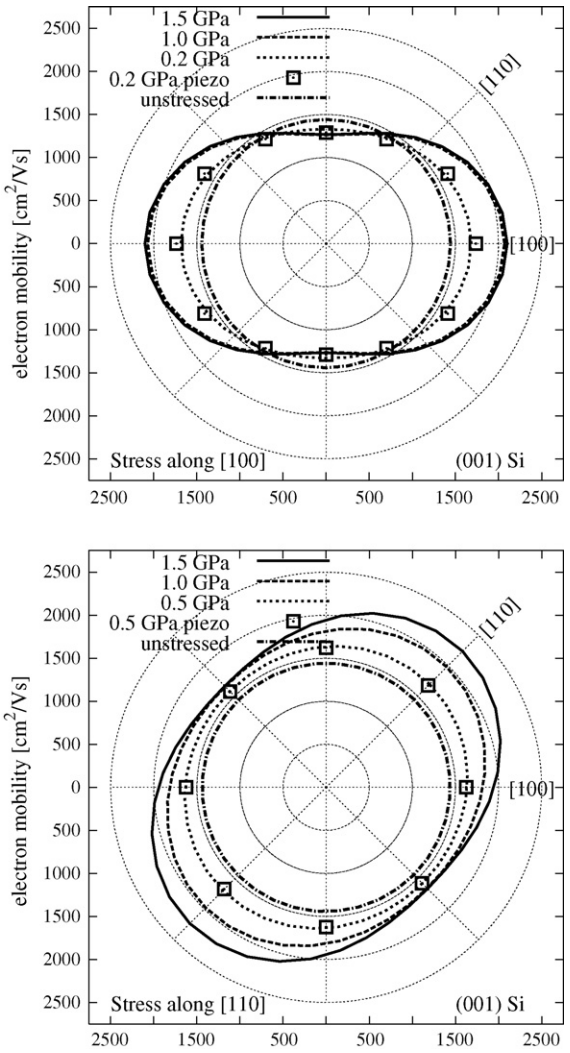

Fig. 5. Mobility enhancement for different levels of uniaxial tensile stress along [1 1 0] and [1 0 0]. The mobility enhancement is also calculated using the piezo coefficients [23].

4. Results

Fig. 4 shows how uniaxial tensile stress along ⟨1 1 0⟩ significantly changes the transversal masses of the Δ_2-valley pair, whereas the mass change for biaxial tensile strain in the {0 0 1}-plane is negligible. These results are in good agreement with a study recently reported in [25]. Additionally, the stress induced effective mass change is found to strongly depend on the internal strain parameter ξ.

We have parameterized the effective mass change of the Δ_2-valley pair observed from EPM calculations

$$m_{t,||} = 0.196 - 0.016P, \qquad m_{t,\perp} = 0.196 + 0.029P, \qquad m_l = 0.914 + 0.0236P^2. \tag{4}$$

Here, m_l denotes the out-of-plane mass, $m_{t,||}$ and $m_{t,\perp}$ the in-plane masses parallel and perpendicular to stress, and P the magnitude of uniaxial stress along ⟨1 1 0⟩ in units of GPa. The direction of stress leads to a pronounced anisotropy of the mobility in the transport plane.

Fig. 5 shows the effect of in-plane stress on a (0 0 1) wafer on the in-plane electron mobility. Uniaxial stress is applied along [1 1 0] and [1 0 0]. Both conditions split the sixfold degenerate Δ_6 valleys in a twofold Δ_2-valley pair and a fourfold Δ_4-valley pair. If stress is applied along [1 1 0], the Δ_2-valley pair moves down in energy, having m_t in the plane of transport. Neglecting the stress induced effective mass change, the in-plane mobility is

enhanced isotropically. Only by taking into account the stress induced effective mass change, the experimentally observed anisotropic mobility enhancement can be reproduced by simulation. For small stress, where the mobility enhancement can also be modeled using the piezo coefficients, good agreement between the two models is found.

When stress is applied along [1 0 0], the Δ_4-valley pairs (orientated along [0 0 1] and [0 1 0]) move down in energy. These valleys have the transport mass m_t in the stress direction, but in the in-plane direction [0 1 0], the valley along [0 1 0] has a mass of m_l, thus the mobility is lowered in this direction.

5. Conclusions

The nonlocal empirical pseudopotential method has been generalized to incorporate strain effects arising from uniaxial stress. Symmetry considerations can be exploited to deduce volume and shape of the irreducible wedge under stress along ⟨1 0 0⟩, ⟨1 1 1⟩, and ⟨1 1 1⟩. Our results for the Si band structure confirm the experimentally observed warping of the conduction band [4,8,18,25], when uniaxial tensile stress is applied along ⟨1 1 0⟩. It is demonstrated that accurate models for the electron mobility in uniaxially stressed Si need to take into account the electron effective mass change.

Acknowledgment

This work has been partly supported by the Austrian Science Fund (FWF), project 17285-N02.

References

[1] J.R. Chelikowsky, M.L. Cohen, Nonlocal pseudopotential calculations for the electronic structure of eleven diamond and zinc-blende semiconductors, Phys. Rev. B 14 (2) (1976) 556–582.
[2] M.V. Fischetti, S.E. Laux, Band structure, deformation potentials, and carrier mobility in strained Si, Ge, and SiGe alloys, J. Appl. Phys. 80 (4) (1996) 2234–2252.
[3] P. Friedel, M.S. Hybertsen, M. Schlüter, Local empirical pseudopotential approach to the optical properties of Si/Ge superlattices, Phys. Rev. B 39 (11) (1989) 7974–7977.
[4] J.C. Hensel, H. Hasegawa, M. Nakayama, Cyclotron resonance in uniaxially stressed silicon. ii. Nature of the covalent bond, Phys. Rev. 138 (1A) (1965) A225–A238.
[5] C. Herring, E. Vogt, Transport and deformation-potential theory for many-valley semiconductors with anisotropic scattering, Phys. Rev. 101 (3) (1956) 944–961.
[6] J. Hinckley, J. Singh, Influence of substrate composition and crystallographic orientation on the band structure of pseudomorphic Si–Ge alloy films, Phys. Rev. B 42 (1990) 3546–3566.
[7] M. Horstmann, A. Wei, T. Kammler, J. Höntschel, H. Bierstedt, T. Feudel, K. Frohberg, M. Gerhardt, A. Hellmich, K. Hempel, J. Hohage, P. Javorka, J. Klais, G. Koerner, M. Lenski, A. Neu, R. Otterbach, P. Press, C. Reichel, M. Trentsch, B. Trui, H. Salz, M. Schaller, H.-J. Engelmann, O. Herzog, H. Ruelke, P. Hübler, R. Stephan, D. Greenlaw, M. Raab, N. Kepler, Integration and optimization of embedded-SiGe, compressive and tensile stressed liner films, and stress memorization in advanced SOI CMOS technologies, in: Proc. Intl. Electron Devices Meeting, 2005.
[8] H. Irie, K. Kita, K. Kyuno, A. Toriumi, In-plane mobility anisotropy and universality under uni-axial strains in n- and p-MOS inversion layers on (1 0 0), (1 1 0), and (1 1 1) Si, in: Proc. Intl. Electron Devices Meeting, 2004.
[9] C. Jacoboni, L. Reggiani, The Monte Carlo method for the solution of charge transport in semiconductors with applications to covalent materials, Rev. Mod. Phys. 55 (3) (1983) 645–705.
[10] C.-H. Jan, P. Bai, J. Choi, G. Curello, S. Jacobs, J. Jeong, K. Johnson, D. Jones, S. Klopcic, J. Lin, N. Lindert, A. Lio, S. Natarajan, J. Neirynck, P. Packan, J. Park, I. Post, A 65 nm ultra low power logic platform technology using uni-axial strained silicon transistors, in: Proc. Intl. Electron Devices Meeting, 2005.
[11] L. Kleinman, Deformation potentials in silicon. I. Uniaxial strain, Phys. Rev. 128 (6) (1962) 2614–2621.
[12] L. Kleinman, J.C. Phillips, Crystal potential and energy bands of semiconductors. III. Self-consistent calculations for silicon, Phys. Rev. 118 (5) (1960) 1153–1167.
[13] G. Kresse, J. Furthmüller, Efficiency of ab-initio total energy calculations for metals and semiconductors using a plane-wave basis set, Comput. Mater. Sci. 6 (1996) 15–50.
[14] G. Kresse, J. Furthmüller, Efficient iterative schemes for ab initio total-energy calculations using a plane-wave basis set, Phys. Rev. B 54 (16) (1996) 11169–11186.
[15] G. Kresse, J. Hafner, Ab initio molecular dynamics for liquid metals, Phys. Rev. B 47 (1) (1993) 558–561.
[16] G. Kresse, J. Hafner, Ab initio molecular-dynamics simulation of the liquid-metal amorphous-semiconductor transition in germanium, Phys. Rev. B 49 (20) (1994) 14251–14269.
[17] G. Kresse, D. Joubert, From ultrasoft pseudopotentials to the projector augmented-wave method, Phys. Rev. B 59 (3) (1999) 1758–1775.

[18] L.D. Laude, F.H. Pollak, M. Cardona, Effects of uniaxial stress on the indirect exciton spectrum of silicon, Phys. Rev. B 3 (8) (1971) 2623–2636.
[19] O. Madelung, Semiconductors: Data Handbook, Data in Science and Technology, 3rd ed., Springer, 2003.
[20] O. Nielsen, R. Martin, Stresses in semiconductors: ab initio calculations on Si, Ge, and GaAs, Phys. Rev. B 32 (6) (1985) 3792–3805.
[21] J.C. Phillips, Energy-band interpolation scheme based on a pseudopotential, Phys. Rev. 112 (3) (1958) 685–695.
[22] M.M. Rieger, P. Vogl, Electronic-band parameters in strained $Si_{1-x}Ge_x$ alloys on $Si_{1-y}Ge_y$ substrates, Phys. Rev. B 48 (19) (1993) 14276–14287.
[23] C.S. Smith, Piezoresistance effect in germanium and silicon, Phys. Rev. 94 (1) (1954) 42–49.
[24] S.-E. Thompson, M. Armstrong, C. Auth, M. Alavi, M. Buehler, A 90-nm logic technology featuring strained-silicon, IEEE Trans. Electron Devices 51 (11) (2004) 1790–1797.
[25] K. Uchida, T. Krishnamohan, K. Saraswat, Y. Nishi, Physical mechanisms of electron mobility enhancement in uniaxial stressed MOSFETs and impact of uniaxial stress engineering in ballistic regime, in: Proc. Intl. Electron Devices Meeting, 2005.
[26] C.G. Van de Walle, R.M. Martin, Theoretical calculations of heterojunction discontinuities in the Si/Ge system, Phys. Rev. B 34 (8) (1986) 5621–5634.
[27] VMC2.0, Vienna Monte Carlo 2.0 User's Guide, Institut für Mikroelektronik, http://www.iue.tuwien.ac.at/software, Technische Universität Wien, Austria, 2006.